

Temperature and density dependence of ^{129}Xe chemical shift in xenon gas

Cynthia J. Jameson, A. Keith Jameson, and Sheila M. Cohen

*Department of Chemistry, University of Illinois at Chicago Circle, Chicago, Illinois 60680**Loyola University, Chicago, Illinois 60626*

(Received 6 April 1973)

Studies of density dependence of ^{129}Xe chemical shift in xenon gas at room temperature have shown that while the chemical shielding does have quadratic and cubic dependence on density over densities up to 250 amagat, $\sigma(\rho, T) = \sigma_0 + \sigma_1(T)\rho + \sigma_2(T)\rho^2 + \sigma_3(T)\rho^3$, the curve is essentially linear up to about 100 amagat. We have now obtained $\sigma_1(T)$, the linear density coefficient of chemical shielding, for pure xenon over the temperature range 240–440 °K. The experimental values of $\sigma_1(T)$ can be fitted by a fourth degree polynomial: $\sigma_1(\tau) = 0.536 - 0.135 \times 10^{-2}\tau + 0.132 \times 10^{-4}\tau^2 - 0.598 \times 10^{-7}\tau^3 + 0.663 \times 10^{-10}\tau^4$ (ppm/amagat), where $\tau = T - 300$ °K. Comparison is made with $\sigma_1(T)$ for other nuclei and with $\sigma_1(T)$ predicted by various theoretical models.

Previous ^1H , ^{19}F , and ^{129}Xe NMR studies on gaseous systems show that the chemical shift has an essentially linear dependence on density up to densities of about 100 amagat.^{1,2} This implies that at these densities the interactions which are important are binary. Precise measurements of ^{129}Xe chemical shifts over a larger density range showed that higher order terms become important.^{1,3} The virial coefficients of chemical shielding at room temperature have been reported for Xe in xenon gas of densities of 30 up to 250 amagat¹ as

$$\sigma(\rho, T) = \sigma_0 + \sigma_1(T)\rho + \sigma_2(T)\rho^2 + \sigma_3(T)\rho^3,$$

where, at room temperature,

$$\sigma_1 = -0.548 \pm 0.004 \text{ ppm/amagat},$$

$$\sigma_2 = (-0.169 \pm 0.02) \times 10^{-3} \text{ ppm/amagat}^2,$$

$$\sigma_3 = (0.163 \pm 0.01) \times 10^{-5} \text{ ppm/amagat}^3.$$

This work is on the experimental determination of $\sigma_1(T)$ for pure xenon over the temperature range 240–440 °K. Accurate temperature dependence of σ_1 is essential in the determination of the functional form of chemical shielding of two interacting molecules since

$$\sigma_1(T) = 4\pi \int_0^\infty \sigma(R) \exp[-U(R)/kT] R^2 dR$$

for spherically symmetric molecules such as Xe. Previous interpretation of $\sigma(R)$ in terms of a sum of contributions due to neighbor-molecule magnetic anisotropy, polar contributions, van der Waals and repulsive interactions, has been modestly successful in the case of ^1H and ^{19}F , and less so in the case of ^{129}Xe . Part of the difficulty may have been the lack of good potential functions for the pair of molecules under consideration. The rest may be due to the semiquantitative, albeit intuitive models used for the different contributions. In order to have a check on the validity of these models, it would be necessary to have a directly-determined functional form for $\sigma(R)$. This is possible if $\sigma_1(T)$

can be determined reasonably precisely over a wide range of temperatures for a gas whose intermolecular potential is likewise precisely determined. The latter criterion suggests a rare gas. The only one of these for which nuclear parameters are suitable is xenon. It has a high natural abundance (26.24%) of the spin $\frac{1}{2}$ isotope. It has a wide range of chemical shifts (about two orders of magnitude greater than for ^1H). The intermolecular potential for Xe–Xe has been obtained recently by fitting differential cross section data and second virial coefficients. This Xe₂ potential is of piecewise analytic form.⁴ Having so defined the kernel $[\exp(-U(R)/kT)]$ in this Fredholm integral equation of the first kind,

$$\sigma_1(T) = 4\pi \int_0^\infty \sigma(R) \exp[-U(R)/kT] R^2 dR,$$

one then only needs precise data points for $\sigma_1(T)$ in order to carry out a numerical solution for $\sigma(R)$. This study is a determination of $\sigma_1(T)$ for pure xenon over the temperature range 240–440 °K using samples of xenon gas varying in density from 19 to 122 amagat.

EXPERIMENTAL

Samples of volume ~ 0.07 ml were made in 3.9 mm o.d., 1.2 mm i.d. borosilicate tubing with a length of about 5 cm. They were calibrated, filled and sealed off by the method previously described.¹ The volume of these tubes could be precisely determined to within 1%. In addition the sample tubes were cracked open after all spectroscopic measurements had been carried out and the volumes were measured using mercury. This leads to somewhat more accurately determined densities. The change in volume of borosilicate tubing over the temperature range 250–440 °K due to thermal expansion is less than 0.1% and hence was neglected. The samples were preheated to temperatures above those which could be reached in the probe at the high temperature studies, in order to preclude explosions

inside the probe due to weak seals or strains in the glass. All samples survived this preheating. These samples of xenon fit into standard thin-walled 5 mm o.d. NMR tubes with enough annular space for the lock substance. The sample tubes are sufficiently short so as to have uniformity in temperature over the entire length of the tube.

All NMR measurements were made on a Bruker HFX90 variable frequency spectrometer operating at a nominal field strength of 21.15 kG, at which field the ^{129}Xe resonance frequency is 24.89 MHz.

The long term stability of the magnetic resonance system was enhanced by using as a mixing frequency the output frequency of a Schmondl frequency synthesizer, which was externally locked to the 1-MHz master crystal of the spectrometer, instead of that supplied by the ^{129}Xe -frequency quartz oscillator. The xenon resonance frequencies were read directly at the transmitter output using an electronic frequency counter. The magnetic field was stabilized on the ^{19}F or ^1H resonance signal of a liquid lock substance suitable for the temperature range to be covered.

In order to cover the entire temperature range of interest here, that is, from about 200 °C down to the point of liquefaction of the sample, it was necessary to use three different lock compounds: (1) In the low temperature region, i.e., up to about 300 °K, the magnetic field was stabilized on the proton resonance signal of TMS. For measurements throughout this temperature region, the field strength was adjusted so that the proton signal from TMS could be observed at exactly 90.010415 MHz. (2) To cover the temperature interval of approximately 280–340 °K, the field was locked to the ^{19}F resonance signal of hexafluorobenzene, observed at exactly 84.678687 MHz. (3) In the high temperature interval, i.e., from 350–440 °K, 1,4-dibromotetrafluorobenzene was employed as the lock compound. Here the field strength was adjusted so that the first high-field audio sideband (modulation frequency = 3.9 kHz) of the ^{19}F resonance frequency of the reference compound could be observed at exactly 84.678687 MHz. Thus, resonance frequencies in region (2) are shifted by approximately 19.5 ppm to low field when compared with the corresponding frequencies in region (1); in region (3) the shift is approximately 11 ppm to low field when compared with region (1).

The observation of xenon gas in natural abundance is, not surprisingly, complicated by sensitivity problems, attributable, for the most part, to the long ^{129}Xe relaxation time in a gas of modest density, the low filling factor imposed by safety considerations, and the low sensitivity of ^{129}Xe nuclei. These familiar problems were largely circum-

vented by use of signal averaging of the cw NMR ^{129}Xe spectra to improve the signal to noise ratio. Using this signal enhancement technique, we could routinely take spectra of low-density pure xenon samples (30 amagat or less) without recourse to the previously used procedure of adding known small amounts of O_2 to samples to shorten T_1 .¹ The frequency sweep of the spectrometer measuring channel was controlled by a minicomputer which also provided the control voltage of the x-y flat bed recorder so that a fixed coupling between the frequency axis and the x axis of the recorder is achieved. Depending on the density of xenon in the sample, a signal to noise ratio of 8 to 1 or better was obtained in 2 to 64 scans. The spectrum is then read out onto the recorder and the frequency at the center of the signal is measured with a frequency counter. As a cursory check, the frequency difference between the stabilization peak and the measured peak is read off the spectrometer frequency counter. The resonance frequency at various temperatures and densities occurred over a 2000 Hz range.

Regulation of the temperature of the spinning 5-mm sample assembly (gas sample tube together with lock substance in the annular region) was provided by a Bruker B-ST 100/700 variable temperature system. This digital unit has a three-decade digital indicator to select the temperature and a meter to indicate the deviations from this value. The meter can be read to the nearest 0.1 deg. The heat exchange gas was nitrogen. This system was carefully calibrated and was found to maintain a selected temperature to within ± 0.2 deg as measured by a copper-constantan thermocouple placed immediately adjacent to the 5-mm tube in high-resolution quartz dewar insert. The regulator was calibrated at the ice point and the linearity of regulator reading with temperature was checked with a sample of methanol in the proton probe insert with the field locked to the CH_3 of CH_3OH . The temperature regulator readings in the xenon probe insert were checked at the boiling points of TMS and hexafluorobenzene and the freezing point of hexafluorobenzene. All subsequent day-to-day checks on the stability and reproducibility of the temperature regulation system were made between samples by repeated measurements at various temperatures on a sample of intermediate density selected as a convenient but otherwise arbitrary temperature standard. We estimate that the absolute temperatures were known to ± 1 °C and the precision was about ± 0.2 °C. The ^{129}Xe resonance frequency was measured at about 5 deg intervals. In each temperature range the signal was located at room temperature (or at 350 °K in the higher temperature range) and the temperature was then set

in 10 deg steps in one direction, then back in 10 deg steps between the previous points in order to minimize systematic errors in the measurements. In the higher temperature region the chemical shifts are not as large as they are at lower temperatures, so the spectrum was taken at 10–15 deg intervals.

RESULTS

Some typical frequency vs temperature curves for samples of given densities are shown in Fig. 1 for the three lock substance temperature ranges. For each lock substance each set of the frequency vs temperature data is fitted in a least squares sense to polynomials of degree 2 and 3. No significant improvement in standard deviation was obtained with degree 3 and no systematic deviations were observed in the fit to degree 2 to indicate the

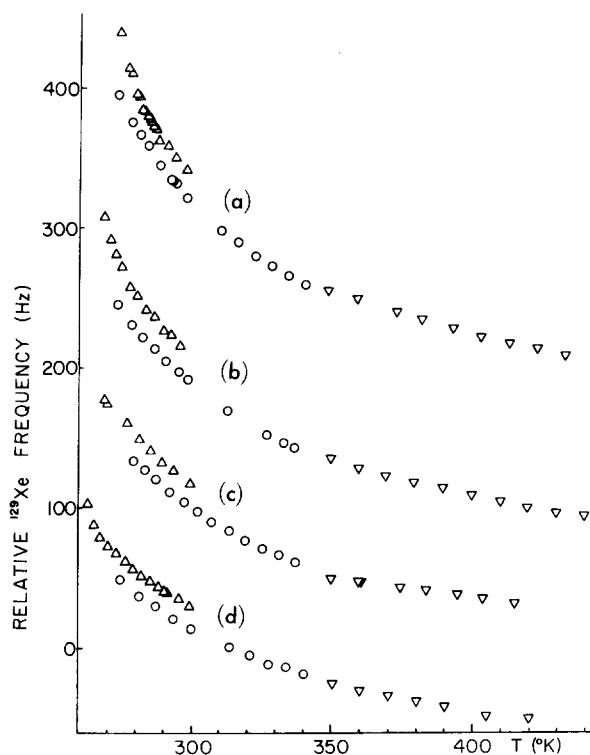


FIG. 1. Temperature dependence of ^{129}Xe frequency observed at 21.15 kG, with field locked on the ^1H signal of TMS from 240 to 300°K, on the ^{19}F signal of hexafluorobenzene from 280 to 340°K, and on the first sideband of dibromotetrafluorobenzene from 350 to 440°K. There are slight differences in field due to stabilizing the field by resonance signals of the different lock substances. The arbitrary zero frequency of the ordinate corresponds to 24.893768 MHz (TMS), 24.893300 MHz (C_6F_6), 24.893578 MHz (DBTFB). The TMS data has been offset by 20 Hz for clarity. Densities of samples are: (a) 71.19 amagat, (b) 57.87 amagat, (c) 47.16 amagat, (d) 37.44 amagat. These are representative of the 12 samples of various densities which were used in this study.

need for a higher degree polynomial. Thus, all the analyses which follow use the results of the fit to a polynomial of degree 2

$$\nu = a_0(\rho) + a_1(\rho)(T - t_0) + a_2(\rho)(T - t_0)^2,$$

where $t_0 = 300^\circ\text{K}$ for the TMS and C_6F_6 ranges and $t_0 = 350^\circ\text{K}$ for the dibromotetrafluorobenzene range. Twenty-seven such curves were so fitted. For each lock substance temperature range, $a_0(\rho)$ vs ρ , $a_1(\rho)$ vs ρ , and $a_2(\rho)$ vs ρ were plotted. Only the latter showed any departure from linearity outside of experimental error. This was borne out by attempts to fit $a_0(\rho)$ vs ρ and $a_1(\rho)$ vs ρ to both first degree and second degree polynomials. Thus, for each temperature range we were able to determine all the parameters in the equation

$$\begin{aligned} \nu = & (a_0^{(0)} + a_0^{(1)}\rho) + (a_1^{(0)} + a_1^{(1)}\rho)(T - t_0) \\ & + (a_2^{(0)} + a_2^{(1)}\rho + a_2^{(2)}\rho^2)(T - t_0)^2. \end{aligned}$$

These parameters are given in Table I. The lock substance itself has a temperature dependence which is obtained by taking the limit of ν as the density of xenon, ρ , approaches zero. These results do not affect the $\sigma_1(T)$ data directly and are reported elsewhere.⁵

Note that the above equation is only valid for each temperature range and only for low density samples. For high density samples, the quadratic dependence on density, $\sigma_2(T)$, may not be negligible. Possible evidence for this will be discussed later.

The difference between $a_0^{(0)}$ for C_6F_6 and $a_0^{(0)}$ for tetramethylsilane at 300°K is due to the field being slightly different when locked to ^1H in TMS than when locked to ^{19}F in C_6F_6 . Experimentally this is directly obtained from the ^{129}Xe frequency at 300°K of the same sample, with different lock substances. This difference was observed for TMS and C_6F_6 at 300°K to be 478 Hz. Similarly, for C_6F_6 data extrapolated 10 deg to 350°K and compared with that for dibromotetrafluorobenzene first high-field sideband at 350°K, this difference was observed to be 280 Hz. The difference between the intercepts obtained from $a_0^{(0)}(\text{C}_6\text{F}_6) = 24\,892\,809.4$ Hz and $a_0^{(0)}(\text{TMS}) = 24\,893\,287.6$ Hz is indeed 478 Hz, in agreement with what was observed. This indicates that the polynomial fitted curves accurately reproduced the temperature intercept of experimental data (300°K). Comparison with the observed 280 Hz difference between the C_6F_6 and the dibromotetrafluorobenzene data is a little more involved since the t_0 used for the C_6F_6 data was 300°K but the t_0 used for the dibromotetrafluorobenzene was 350°K. The temperature dependence of C_6F_6 itself is involved in this. The $a_0^{(0)}$ of the dibromotetrafluorobenzene data does come within 2 Hz of the $(a_0^{(0)} + 50a_1^{(0)} + 2500a_2^{(0)})$ for C_6F_6 plus 280 Hz. When one

TABLE I. Temperature coefficients of ^{129}Xe frequency: $\nu(T) = a_0^{(0)} + a_0^{(1)}\rho + \{a_1^{(0)} + a_1^{(1)}\rho\}(T - t_0) + \{a_2^{(0)} + a_2^{(1)}\rho\}(T - t_0)^2$.^a

Lock Substance	t_0 (°K)	$a_0^{(0)}$	$a_1^{(0)}$	$a_2^{(0)}$	$a_0^{(1)}$	$a_1^{(1)}$	$a_2^{(1)}$
C_6F_6	300	24892809.4	+0.28695	-0.005167	13.3382	-0.03643	+0.000339
TMS	300	24893287.6	+0.09400	-0.004896	13.389	-0.0243	+0.00066
DBTFB	350	24893088.6	-0.08711	+0.000927	12.326	-0.00848	+0.000013

^aThe units all involve Hz, amagat, and °K.

considers the uncertainty in the temperature dependence of C_6F_6 itself, this is close enough. As was found in earlier work, plots of frequency vs density at a given temperature were linear within experimental error for densities of about 100 amagat or less. Examples of such plots are shown in Fig. 2. The temperature dependence of the intercept is due to the lock substance resonance frequency varying with temperature. An analysis of this lock substance temperature dependence is reported elsewhere.⁵

A computer program was written which stepped through temperature, and for each temperature fitted the frequencies vs density to a straight line. The slope gives σ_1 at that temperature. This was done for each temperature range (and lock substance.) The resulting values are shown in Table II and plotted in Fig. 3. There is no minimum observed in the temperature range which has been covered. However, this does not preclude the presence of a minimum at some much higher temperature. Fitting $\sigma_1(T)$ to a polynomial of degree 4

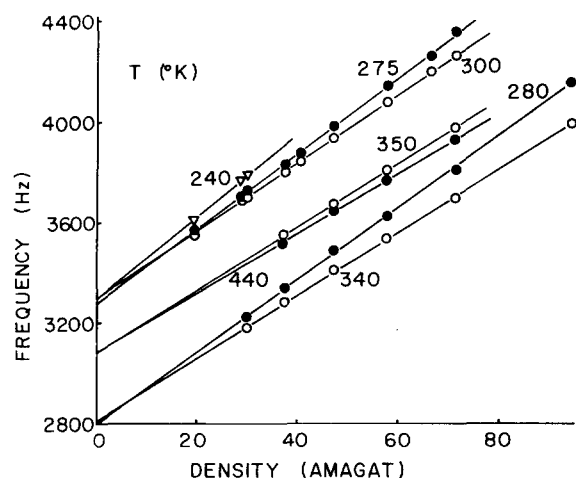


FIG. 2. Density dependence of ^{129}Xe frequency at selected temperatures in the range 240–300 °K, 280–340 °K, and 350–440 °K, using the ^1H signal of TMS, the ^{19}F signal of C_6F_6 and the ^{19}F signal of dibromotetrafluorobenzene, respectively, for field stabilization. ^{129}Xe frequencies = 24 890 000 + ordinate. The differences in intercept are discussed in the text.

gives

$$\sigma_1(\tau) = 0.536 - 0.135 \times 10^{-2} \tau + 0.132 \times 10^{-4} \tau^2 - 0.598 \times 10^{-7} \tau^3 + 0.663 \times 10^{-10} \tau^4 \text{ ppm/amagat},$$

where $\tau = T - 300$ °K. Terms up to at least τ^3 are needed to obtain a reasonable fit, but probably the quartic term should be included since it leads to less systematic deviation in σ_1 at the low and high temperature ends of each range.

In the lowest temperature range (TMS lock), not all samples could be used throughout the entire temperature range because at some temperature, depending on the xenon density, the liquid-vapor coexistence curve for xenon is reached and condensation occurs. Thus, samples at densities greater than 66 amagat could not be included below 275 °K,

TABLE II. Temperature dependence of second virial coefficient of chemical shielding, σ_1 , for ^{129}Xe in xenon gas.

T, °K	σ_1 (Hz/amagat)		
	with TMS lock	with C_6F_6 lock	with DBTFB lock
240	16.88		
245	16.45		
250	16.05		
255	15.66		
260	15.31		
265	14.98		
270	14.68		
275	14.40		
280	14.15	14.20	
285	13.92	13.96	
290	13.72	13.74	
295	13.55	13.53	
300	13.40	13.34	
305		13.16	
310		13.01	
315		12.87	
320		12.74	
325		12.64	
330		12.55	
335		12.48	
340		12.42	
350			12.33
360			12.24
370			12.16
380			12.08
390			12.01
400			11.94
410			11.86
420			11.80
430			11.73
440			11.67

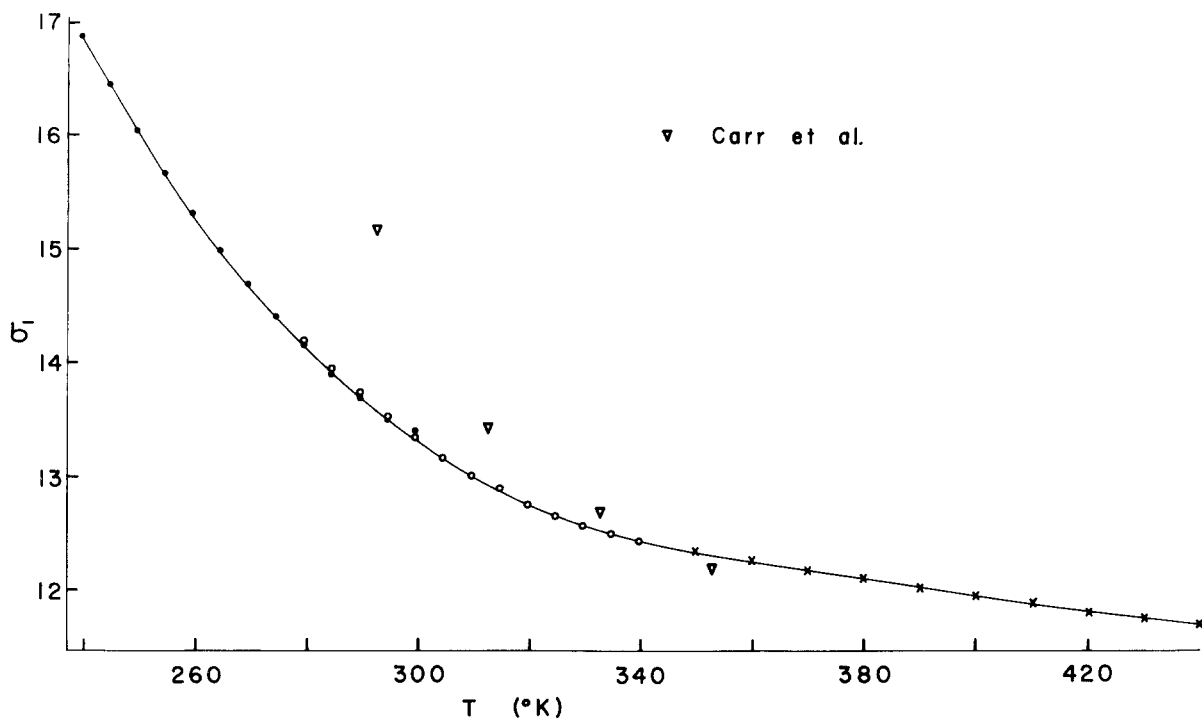


FIG. 3. Temperature dependence of the second virial coefficient of chemical shielding, $\sigma_1(T)$ for ^{129}Xe in pure xenon gas. \bullet , the TMS range; \circ , the C_6F_6 range; and \times , the DBTFB range. Values of σ_1 reported by Kanegsberg, Pass, and Carr³ (∇) are also shown for comparison.

samples greater than 47 amagat could not be included below 265 °K and those with densities greater than 37 amagat could not be included below 260 °K. For these low density samples very near the condensation temperature, the σ_2 and higher contributions are definitely no longer negligible. When the higher density samples are included in the data analysis, there is a systematic deviation of "apparent σ_1 " as the temperature decreases showing the increasing contribution of the $\sigma_2\rho^2$ and possibly other higher terms. This deviation is consistently

on the concave side of the σ_1 curve, implying the sign of σ_2 to be the same as that of σ_1 . Thus, analysis of the data below 300 °K to yield an estimate of σ_2 was attempted. The same computer program was used to fit the ratio of frequency difference (observed frequency minus the frequency extrapolated to zero density) to density versus density for each temperature. The five lower density points were used to obtain $\nu_{\rho=0}$ and all nine densities up to 71 amagat were used for a least squares fit to the linear equation

$$(\nu - \nu_{\rho=0})/\rho = \sigma_1 + \sigma_2\rho$$

The slope gives an estimate of the third virial coefficient of chemical shielding at various temperatures. The $\sigma_2(T)$ estimated in this manner are shown in Table III and plotted in Fig. 4.

DISCUSSION

Our earlier data on σ_1 at room temperature compares favorably with that obtained in this study:

$$\text{Ref. 1: } (T \sim 298 \pm 2) \sigma_1 = -0.548 \pm 0.004 \text{ ppm/amagat,}$$

$$\text{this work: } (T = 298) \sigma_1 = -0.539 \text{ ppm/amagat.}$$

The minus sign is used to indicate a downfield shift. The ± 0.004 was of course an indication of the standard deviation of the least squares fitted

TABLE III. Temperature dependence of the third virial coefficient of chemical shielding, σ_2 , for ^{129}Xe in xenon gas.

T °K	σ_2 (Hz amagat ⁻²)
250	3.54×10^{-2}
255	2.88
260	2.29
265	1.78
270	1.35
275	1.00
280	0.72
285	0.52
290	0.40
295	0.36
300	0.39

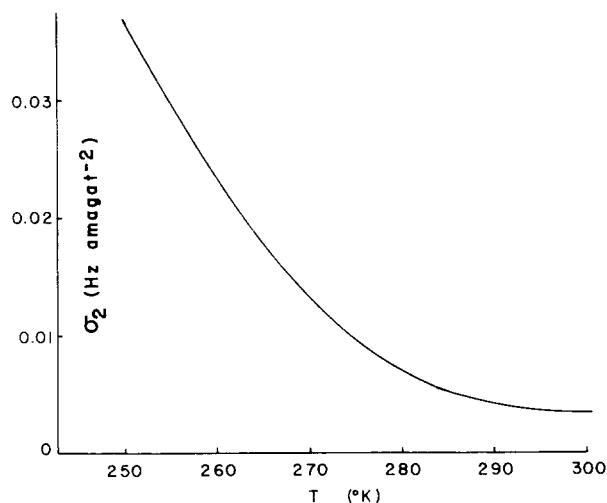


FIG. 4. Temperature dependence of the third virial coefficient of chemical shielding, $\sigma_2(T)$, estimated for ^{129}Xe in xenon gas.

data and not necessarily an indication of accuracy.

Kanegsberg, Pass and Carr have reported σ_1 and σ_2 for pure xenon.³ The interpretation of their data is somewhat different from ours. While they used only two samples with densities lower than 100 amagat, we have used in both our previous work and this one, a large number of low density samples. The experimental points in Fig. 1 of Ref. 3 appear to be consistent with ours. However, their fitted curve shows considerably more curvature in the lower density region than would seem to be indicated by their lower density points and ours. Thus, their values of σ_1 are somewhat higher than ours and are shown in Fig. 3, for comparison.

In any data analysis which involves a fit to a polynomial series there is usually some coupling between the terms, especially of adjacent order. Because of truncation and because the experimental data points are not mathematically exact but have some associated error the use of higher order terms can compensate for deficiencies in the coefficients of lower order terms, all within experimental error. Thus, usually a unique fit can not be obtained. This is one of the problems which accompanies determination of many properties such as the second and higher order virial coefficients in gases. The same holds true for the virial coefficients of chemical shielding. The difference between Carr's work and ours is of this nature. Although their experimental points are not inconsistent with ours, their fitted polynomial is not identical to ours. The major difference lies in the exaggerated curvature in their polynomial function (but not in their experimental points) between 0 and 100 amagat. They have only two points in this den-

sity range whereas we had 8 in our previous study and 12 in this one. With our better precision and considerably larger number of samples at the lower densities, we find that their polynomial function gives systematic deviations outside of experimental error in this density range. The σ_2 which we obtained in our previous work is probably to some extent coupled to and compensated for by the cubic term $\sigma_3\rho^3$ —especially in densities up to 250 amagat. However, at lower densities, the $\sigma_3\rho^3$ term should be less important, and possibly a somewhat better value for σ_2 could be obtained, especially at the lower temperatures.

Since the primary purpose of this work was to determine $\sigma_1(T)$, no densities greater than about 120 amagat were employed. In fact $\sigma_1(T)$ was obtained only from samples of densities of about 90 amagat or less. Such modest densities preclude determination of σ_2 with any great accuracy or precision. Nevertheless, the values obtained here (see Table III) show (perhaps fortuitously) reasonable agreement with the value of σ_2 obtained at room temperature in previous work.¹ Our previous work, using densities up to 250 amagat, gave a value of $(-0.169 \pm 0.02) \times 10^{-3}$ ppm amagat⁻² at a nominal temperature of 298 °K, in reasonable agreement with our new results of -0.161×10^{-3} ppm amagat⁻². (The minus sign is used to indicate a downfield shift.) Since these values of σ_2 were not obtained in a manner internally consistent with σ_1 they could be in considerable error, perhaps by a factor of two. However, there seems to be no doubt regarding the sign of σ_2 relative to σ_1 .

Adrian⁶ calculated a change of Xe σ_1 over the temperature range 231–347 °K of 4.13×10^{-4} ppm amagat⁻¹ · deg⁻¹. This could be compared with our 18×10^{-4} ppm amagat⁻¹ · deg⁻¹ over 240–340 °K. Adrian's model predicts a smaller change of σ_1 with temperature than is actually observed. He also predicts a minimum at about 580 °K. Our data do not preclude a minimum at temperatures much higher than 440 °K. Using the Raynes, Buckingham, and Bernstein model² we had previously calculated a temperature dependence of σ_1 for Xe equal to 4.03×10^{-4} ppm amagat⁻¹ · degree⁻¹ over the temperature range 240–340 °K.⁷ This could likely be significantly improved by the use of a more realistic potential than the Lennard-Jones but we defer such refinements for comparison with the results of the direct inversion of this $\sigma_1(T)$ data.⁸

Comparison With Temperature Dependence of σ_1 in Other Systems

A nonlinear temperature dependence of σ has been reported for ^{19}F in SiF_4 , CF_4 , and SF_6 ,⁹ and in mixtures of these with other gases.¹⁰ σ_1 in CF_4 changed roughly about 0.7×10^{-4} ppm amagat⁻¹ · deg⁻¹ over

the range 240–340 °K, SiF_4 changed about 1.6×10^{-4} ppm amagat $^{-1} \cdot \text{deg}^{-1}$ over the same range and SF_6 changed about 1.1×10^{-4} ppm amagat $^{-1} \cdot \text{deg}^{-1}$ over the range 270–350 °K. For CF_4 Meinzer¹¹ reports a change in ^{19}F σ_1 of 0.5×10^{-4} ppm amagat $^{-1} \cdot \text{deg}^{-1}$ over the range 302–345 which is consistent with Mohanty and Bernstein's results of 0.7×10^{-4} , since the curve is steeper from 240 to 300 than from 300 to 340 °K. For the other fluoromethanes Meinzer found that the ^{19}F σ_1 changed with temperature by $(0.46, 0.42, \text{ and } 1.41) \times 10^{-4}$ ppm amagat $^{-1} \cdot \text{deg}^{-1}$ in CHF_3 , CH_2F_2 , and CH_3F , respectively, over the temperature range of 302 to 350 °K. In contrast, over the same range (240–340 °K) as the CF_4 and SiF_4 data, pure Xe changed about 18×10^{-4} ppm amagat $^{-1} \cdot \text{deg}^{-1}$. Thus, xenon which has previously been noted as having from 27 to 46 times as large σ_1 values as these gases at 300 °K also has a temperature dependence which is about 11 to 26 times as large as the temperature dependence of these gases.

Linear temperature dependence of ^1H σ_1 has been reported in ethane by Rummens¹² and Meinzer¹¹ in $\text{CH}_n\text{F}_{4-n}$ ($n=1$ to 4). In methane itself, Meinzer found the $\partial\sigma_1/\partial T$ to be very small, 0.66×10^{-6} ppm amagat $^{-1} \cdot \text{deg}^{-1}$ over the temperature range of 302 to 350 °K. In ethane it was 1.87×10^{-6} ppm amagat $^{-1} \cdot \text{deg}^{-1}$.¹² The fluoromethanes had larger temperature coefficients: $(0.16 \text{ to } 0.24) \times 10^{-4}$ ppm amagat $^{-1} \cdot \text{deg}^{-1}$ over 302 to 350 °K. Over the same temperature range Xe has a change in σ_1 of 8.2×10^{-4} ppm amagat $^{-1} \cdot \text{deg}^{-1}$ which is three orders of magnitude larger than the ^1H methane and ethane temperature shifts. Thus, ^{129}Xe appears to have

a much larger temperature dependence of σ_1 than either the ^{19}F or ^1H systems.

Unlike $B(T^*)$, the second virial coefficient in terms of reduced temperature ($T^* = kT/\epsilon$), the magnitude of $\sigma_1(T^*)$ varies over about three orders of magnitude for the various systems studied so far (^1H , ^{19}F , ^{129}Xe). This indicates that NMR chemical shielding might be a more sensitive probe of certain aspects of intermolecular interactions than conventionally used properties.

ACKNOWLEDGMENT

This work was supported in part by the National Science Foundation (GP-29717).

- ¹A. K. Jameson, C. J. Jameson, and H. S. Gutowsky, *J. Chem. Phys.* **53**, 2310 (1970).
- ²W. T. Raynes, A. D. Buckingham, and H. J. Bernstein, *J. Chem. Phys.* **36**, 3481 (1962).
- ³E. Kanegsberg, B. Pass, and H. Y. Carr, *Phys. Rev. Lett.* **23**, 572 (1969).
- ⁴Y. T. Lee and T. P. Schaefer, *J. Chem. Phys.* (to be published). We wish to thank the authors for private communications of their results.
- ⁵A. K. Jameson and C. J. Jameson, *J. Am. Chem. Soc.* (to be published).
- ⁶F. J. Adrian, *Phys. Rev.* **136**, A980 (1964).
- ⁷Reference 1 and unpublished results of CJJ.
- ⁸C. J. Jameson (unpublished).
- ⁹S. Mohanty and H. J. Bernstein, *Chem. Phys. Lett.* **4**, 575 (1970).
- ¹⁰S. Mohanty and H. J. Bernstein, *J. Chem. Phys.* **54**, 2254 (1971).
- ¹¹R. A. Meinzer, Ph.D. thesis, University of Illinois, Urbana, 1965.
- ¹²F. H. A. Rummens, *Mol. Phys.* **21**, 535 (1971).